Are relay ramps conduits for fluid flow? Structural analysis of a relay ramp in Arches National Park, Utah

ATLE ROTEVATN, HAAKON FOSSEN, JONNY HESTHAMMER, TOR E. AAS & JOHN A. HOWELL

Centre for Integrated Petroleum Research, University of Bergen, Allégaten 41, 5007 Bergen, Norway (e-mail: atle.rotevatn@cipr.uib.no)

Abstract: Relay ramps associated with overlapping faults are commonly regarded as efficient conduits for fluid flow across potentially sealing intra-reservoir fault zones. The current study demonstrates that structural heterogeneity in the often anomalously wide damage zone of relay ramps may represent potential baffles to intra-ramp fluid flow. A network of ramp-parallel, ramp-diagonal and curved cataclastic deformation bands causes compartmentalization of the ramp studied in Arches National Park, Utah. Harmonic average calculations demonstrate that, although single deformation bands have little or no effect on effective permeability, the presence of even a very small number of low-permeable deformation band clusters could reduce along-ramp effective permeability by more than three orders of magnitude. Thus, although relay zones may maintain large-scale geometric communication, the results of this study demonstrate that caution must be exercised when considering relay ramps as fluid conduits across sealing faults in a production situation. Although relay ramps clearly represent effective migration pathways for hydrocarbons over geological time, the extent to which they conduct fluids in a production situation is more uncertain. Quantitative approaches include adjusting the transmissibility multipliers for faults in reservoir models to allow for increased cross-fault flow. If, however, the effect of internal structural heterogeneity is not taken into consideration, this type of adjustment may lead to gross overestimation of the effect of relay ramps. Sedimentology, stratigraphy, burial history and deformation mechanisms are some of the controlling factors for the formation of such structural heterogeneities.

Past work has established that faults may act as barriers to fluid flow in siliciclastic hydrocarbon reservoirs and therefore represent challenges for production. In the recent past, the concepts of fault growth through segment linkage and overlap have received a great deal of attention (Peacock & Sanderson 1991, 1994; Childs *et al.* 1995; Cartwright *et al.* 1996; McLeod *et al.* 2000; Mansfield & Cartwright 2001; Rykkelid & Fossen 2002; Fossen 2003; Peacock 2003; Imber *et al.* 2004). Soft-linked overlapping faults forming relay ramps have been suggested as conductors for fluid flow across fault zones that would otherwise be sealing (Hesthammer & Fossen 1997, 2000; Manzocchi *et al.* 2004). As such, the occurrence and distribution of relay ramps should be an important factor when planning injection and production wells in many faulted reservoirs. A considerable amount of work has contributed to improving our understanding of relay ramp geometry and evolution on a seismically resolvable scale (Peacock & Sanderson 1991, 1994; Imber *et al.* 2004). However, substantial further work is needed to resolve issues concerning internal deformation and distribution of strain within such structures. To aid a better understanding of the effect of relay structures on fluid flow, a structural study has been undertaken in Arches National Park, Utah (Fig. 1).

The main objectives of this paper are to: (1) evaluate the distribution, intensity and mechanisms of deformation within soft-linked relay ramps in porous sandstones; (2) assess the petrophysical implications of the observed internal deformation; and (3) discuss the consequences for fluid flow within relay ramps in porous sandstone reservoirs.

Deformation in porous sandstones

Deformation mechanisms in porous (>15%) sandstones differ from the mechanisms known for non-porous rocks. The pore space within the rock volume allows distinctive processes to take place which accommodate the deformation. These include: (1) grain reorganization resulting in compaction, dilation or no change of volume; and (2) grain crushing (cataclasis) and pore collapse due to stress concentration and failure at the contact points between individual grains (Antonellini *et al.* 1994). The resulting structural

From: LONERGAN, L., JOLLY, R. J. H., RAWNSLEY, K. & SANDERSON, D. J. (eds) *Fractured Reservoirs*. Geological Society, London, Special Publications, **270**, 55–71.
0305-8719/07/$15.00

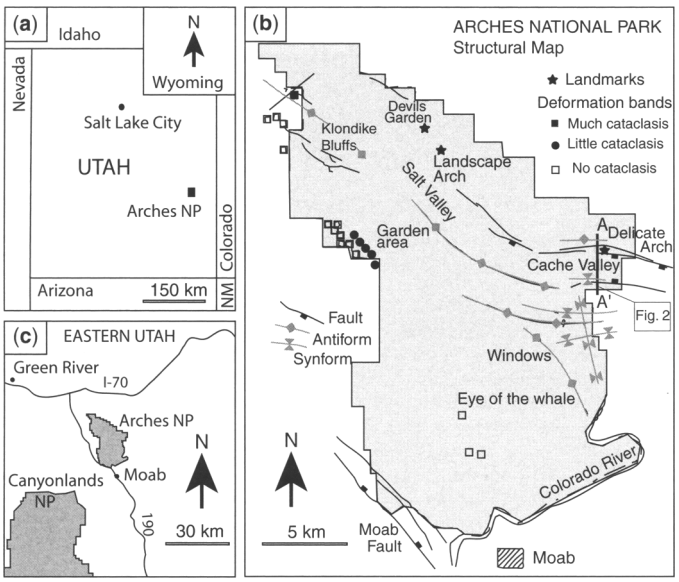

Fig. 1. Maps of (**a**) Utah, (**b**) portion of Eastern Utah and (**c**) structural map of Arches National Park. The latter is based on Antonellini *et al.* (1994). The location of the profile line A–A′ in Figure 2 is indicated.

elements are referred to as deformation bands (Aydin 1978; also known as shear bands, granulation seams and microfaults)–tabular–planar deformation structures along which shear takes place. Deformation bands differ from discrete fault surfaces in a number of ways. Primarily, they do not facilitate a discrete continuous slip plane (microslip planes may exist), but rather a shear zone of less than a few millimetres width. In addition, they typically feature displacement on a millimetre to centimetre scale, and are commonly up to a few metres long. The displacement–length ratio of (cataclastic) deformation bands may be up to three orders of magnitude larger than that known for faults (Fossen & Hesthammer 1997).

The three main types of deformation bands are referred to as disaggregation bands, cataclastic bands, and phyllosilicate bands. The disaggregation type comprises a zone of grain reorganization, but practically no grain crushing. The cataclastic type consists of a core of grain crushing encapsulated in a zone of compaction and grain reorganization (Antonellini *et al.* 1994). Phyllosilicate deformation bands are a special kind of disaggregation band in phyllosilicate-rich sandstones that are also referred to as framework phyllosilicate bands (Knipe 1997). Framework phyllosilicate bands occur in sand and sandstones where phyllosilicate minerals constitute more than *c.* 15% of the mineralogical composition of the sand, and are characterized by alignment of phyllosilicate minerals along the shear plane. The term phyllosilicate smear, on the other hand, refers to shear structures in which the phyllosilicate content is more than 40%, thus featuring a more continuous phyllosilicate membrane that represents a potentially efficient seal against fluid flow.

Deep burial implies higher stress concentrations at grain contact points; thus, cataclasis is more common in porous sandstones having undergone faulting at >1 km depth (Fisher & Knipe 2001). At shallow depths grain reorganization is favoured, and disaggregation bands are commonly found. The deformation bands studied in this work are mainly of the cataclastic type due to the system's relatively deep burial depth at the time of faulting (*c.* 2 km, Davatzes & Aydin 2003). In contrast, those found in many reservoirs offshore Norway are of the disaggregation or phyllosilicate type, owing to shallower, near-surface burial depths at the time of deformation (Knipe 1997; Hesthammer & Fossen 2001).

Aydin and Johnson (1978) realized that faulting in porous sandstones largely follows a three-stage process: (1) as the rock is subjected to stress, individual deformation bands form, and (2) grow to form deformation band cluster zones comprising tens to hundreds of bands. (3) After a period of strain hardening, the rock fails through brittle failure and a discrete slip plane is formed. Hence, the damage zone is formed before the actual fault ruptures. Thus, faults in porous sandstones are commonly accompanied by a damage zone containing deformation bands, as

well as a zone of deformation bands in front of the propagating fault tip. This zone is commonly referred to as the process zone (Cowie & Shipton 1998), or the tip damage zone (Kim *et al.* 2004). The findings of Aydin & Johnson (1978) have been confirmed by a number of field-based (Antonellini & Aydin 1995; Fossen & Hesthammer 1998*a*; Shipton & Cowie 2003) and experimental (Lothe *et al.* 2002; Mair *et al.* 2000) studies.

Previous work has established that sedimentary and structural heterogeneities can reduce the effective permeability of potential reservoir rocks. For example, variability in aeolian cross-bedding can, by itself, reduce effective permeability by at least one order of magnitude (Durlofsky 1992; Weber 1987). In situations where either cataclastic or framework phyllosilicate deformation bands are present, permeability inside deformation bands can be reduced by at 2–6 orders of magnitude relative to that of the surrounding matrix, with the greatest reductions occurring in the most permeable sandstones (Ahlgren 2001; Antonellini & Aydin 1994; Fisher & Knipe 2001; Lothe *et al.* 2002). This reduction is due to the dramatic changes in porosity, pore-throat geometry and pore connectivity caused by grain crushing, compaction and phyllosilicate smear.

Antonellini & Aydin (1994) made mini-permeameter measurements of cataclastic deformation bands in the Jurassic aeolian Entrada sandstone (also studied in this paper, see the next section), and reported 2–3 orders of magnitude permeability reduction. Similarly, Lothe *et al.* (2002) reported permeability reductions at 1–3 orders of magnitude from the early Permian Brumunddal Sandstone (aeolian), SE Norway, based on laboratory flow measurements. Fisher & Knipe (2001) recorded as much as 6-order permeability reduction for cataclastic deformation bands in the aeolian sands of the Permian Rotliegend reservoirs of the Southern North Sea; similarly, a reduction in permeability of up to 6 orders of magnitude was recorded for framework phyllosilicate bands in Brent Group reservoir units in the northern North Sea.

Effective permeability across a bulk volume of rock containing cataclastic deformation bands was addressed theoretically by Sternlof *et al.* (2004), with application to cataclastic deformation band patterns in the Jurassic Aztec Sandstone (aeolian). Their results indicate that a volume fraction of 10% deformation bands would result in at least two orders of magnitude reduction of effective permeability. Deformation bands subjected to cementation are also considered to have a significant negative impact on the effective permeability. Examples of this are found in the northern North Sea, where deformation bands associated with quartz dissolution and precipitation in reservoir rocks that have experienced temperatures of more than 120°C form efficient barriers to fluid flow (Hesthammer *et al.* 2002). Disaggregation bands, however, do not have a considerable impact on the effective permeability (Knipe 1997; Fisher & Knipe 2001).

Study area

The study area is located in the Cache Valley, Arches National Park, SE Utah (Fig. 1) (Doelling 2001). Along the Cache Valley, the porous Entrada Sandstone of the Jurassic San Rafael Group is folded into a rollover anticline in the hanging wall of a major, north-dipping normal fault (Figs 1 & 2). The fault is part of a large fault zone along the Salt and Cache valleys that juxtaposes the lower Jurassic Wingate sandstone in the footwall against the middle-upper Jurassic San Rafael Group and the upper Jurassic–lower Cretaceous Morrison Formation in the hanging wall (Fig. 2; Doelling 1985*a*, *b*). The Entrada sandstone comprises 4–20 m thick, clean, massive aeolian dune units and thinner (1–7 m) and more heterolithic interdune units. The thickness of the section of the Entrada sandstone exposed in the study area is *c.* 80 m. In the Cache Valley, the interval is bisected by antithetic normal faults in the folded hanging wall of the major fault (see above). Some of these faults overlap and form soft-linked relay ramps, one of which has been mapped in detail in order to investigate the distribution of small-scale structures associated with the ramp structure. This ramp (Fig. 3), hereafter referred to as the Delicate Arch Ramp, represents a snapshot in time related to the development of two growing fault segments. Relay ramps generally evolve from (previously underlapping) separate fault segments that overlap to form soft-linked faults (bounding a relay ramp) and ultimately a breached relay (hard-link) when the two fault segments join up (Imber *et al.* 2004). Formation of the Delicate Arch Ramp probably occurred at a depth of *c.* 2 km, before the area was progressively exhumed and finally brought to the current surface (Antonellini & Aydin 1994; Davatzes & Aydin 2003).

A series of regional fracture orientations are displayed in the Salt Valley–Cache Valley area, some at high angles to the fault trends (Fig. 3). Two models have been suggested for the development of these regional fracture networks. Cruikshank and Aydin (1995) suggested that the regional systems of fractures post-date the formation of abundant deformation bands found in the region, and that they have formed after a 95° rotation of the stress field, thereby explaining the high angle to the older structures. Kattenhorn *et al.* (2000) suggested that

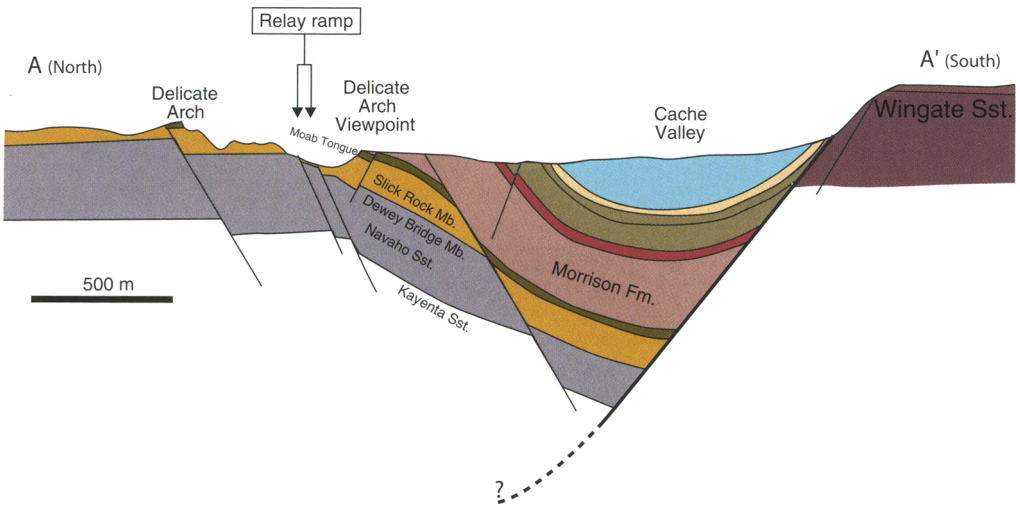

Fig. 2. Geological profile A–A′ across the Cache Valley, showing the orientation of the main fault (in the south), as well as the geometry of the rollover anticline and a drag syncline in the hanging wall to the north of the main fault. Note the predominantly antithetic (with respect to the main fault) normal faults in the hanging wall. South of the Delicate Arch, two closely spaced antithetic normal faults creates a relay ramp. Location of the profile is given in Figure 1. Modified from Antonellini & Aydin (1995).

perturbation of the regional and local stress field (rather than an effective rotation of the entire regional stress field), caused by the numerous fault segments in the valley, may have caused the fracture systems to form at high angles to fault strike. Both models imply that the fractures post-date the faulting and associated deformation band formation, and that fracture formation is probably related to subsequent uplift and exhumation of the crust. As such, the fractures are not directly relevant to relay ramp formation and generalized flow predictions for relay ramps set in subsurface reservoirs. Thus, this issue will not be addressed further herein.

Field observations and collected data

The data collection at the Delicate Arch Ramp was conducted by: (1) systematic structural mapping, where the damage zone structures were mapped in the field onto high-resolution aerial photographs, and (2) structure–frequency profile construction (scanlines), where the intensities of deformation (deformation bands per meter) along north–south orientated profiles were recorded. A total of 23 profiles, with a spacing of 40 m between each profile (totalling nearly 3 km of profiles), were collected. The data are shown in Figure 4, where the frequency profiles have been utilized to construct a deformation band frequency map. The colour codes represent deformation band frequency, whereas the structures drawn on the map represent the main orientations of deformation bands, based on the mapping.

Figure 4 shows a distinct pattern of intensity and orientations, which is described in detail below. Following Kim *et al.* (2004), we distinguish between: (1) linking damage zone (the rock volume affected by fault overlap or linkage); (2) tip damage zone (the damage zone in the continuation of the fault tip); and (3) wall damage zone (describing the footwall and hanging wall damage zone at faults unaffected by fault linkage). The linking damage zone and tip damage zone identified in the study area are described below.

Main faults and tip damage zone

The Delicate Arch relay ramp is bounded by two overlapping E–W-striking normal faults that dip *c.* 70–80° to the south (Figs 3 & 4). The displacement of the northern main fault dies out towards the east, whereas that of the southern fault dies out towards the west (Fig. 5).

The fault core associated with the northern fault is characterized by massive clusters of cataclastic deformation bands (each cluster comprising up to 80–100 bands) and a number of discrete slip planes with pronounced slickenlines. The fault has a displacement of 0–40 m in the ramp area, which increases further west and away from the ramp (Fig. 5). In the ramp area, the northern fault juxtaposes rocks from different stratigraphic levels of the Slickrock Mb,

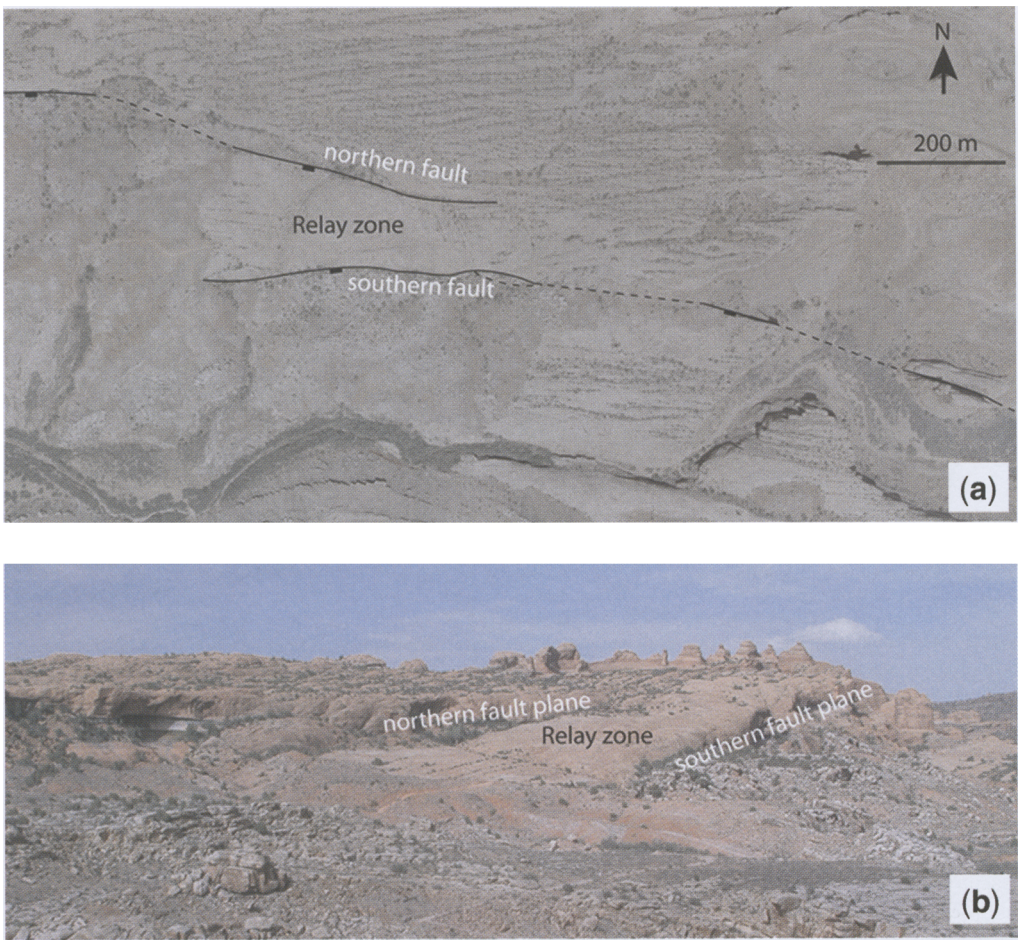

Fig. 3. (**a**) Aerial photo of the Delicate Arch ramp and the surrounding area. The overlapping main faults that bound the ramp are indicated. Note the complex fracture pattern to the north of the ramp. (**b**) Photo of the Delicate Arch ramp. The fault planes of the bounding faults are exposed in the cliff walls adjacent to the ramp. Location of the viewpoint from which the photo was taken is located approximately 500 m west of the south-western corner of the aerial photo in (a).

whereas further west the fault juxtaposes the Slickrock Mb against the Morrison Fm. The fault tip is marked by the termination of discrete slip planes and is well defined in the field. The continuation of the deformation east of the fault tip is characterized by a remarkably continuous tip damage zone (process zone of Cowie & Shipton 1998) of deformation bands that diminishes gradually and terminates *c.* 350 m east of the fault tip. Near the fault tip, the tip damage zone comprises clusters of >40 deformation bands, which split up into smaller clusters and individual deformation bands eastwards along strike. Near the termination of the tip damage zone *c.* 350 m east of the fault tip, only a few small clusters (<10 bands) and individual deformation bands are found. It should be noted that at the fault tip the tip damage zone shifts *c.* 30 m to the north, from where it continues east along the strike of the main fault. The fault core of the southern fault is also characterized by an abundance of deformation bands in large clusters, accompanied by numerous discrete slip planes displaying slickenlines. The southern fault has a displacement of 0–50 m in the ramp area, increasing further east and away from the ramp (Fig. 5). The fault juxtaposes the Slickrock Mb against the Morrison Fm and the top of the Slickrock Mb (Fig. 4). The tip damage zone (process zone) of the southern fault is not exposed and could thus not be mapped and described.

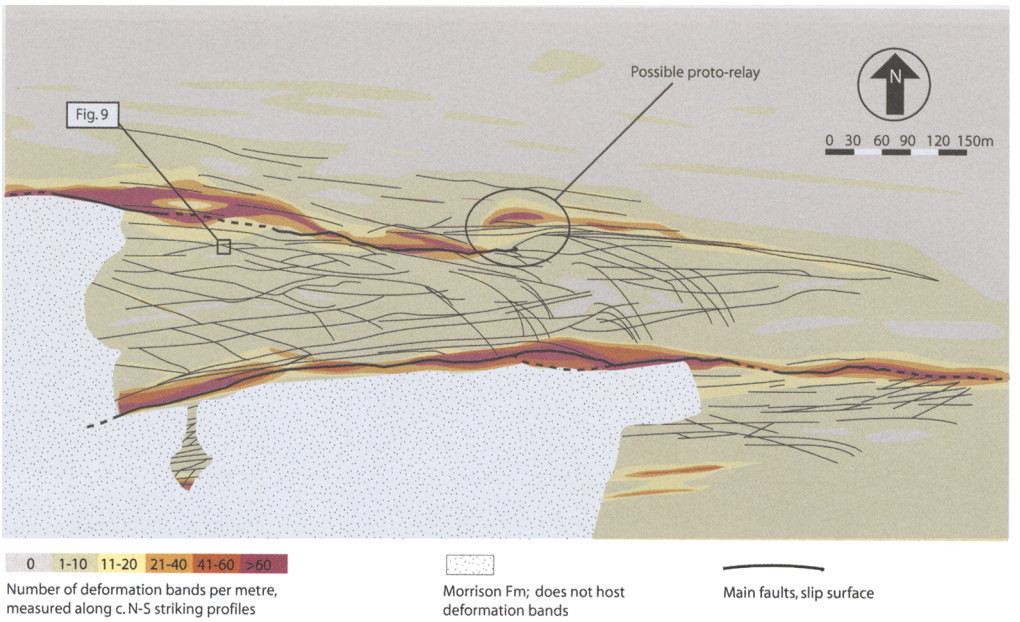

Fig. 4. Map of the Delicate Arch ramp, illustrating the orientation and frequency of deformation bands. Deformation band frequency is represented by colour contours, based on the number of deformation bands per metre recorded along north–south profiles with a profile spacing of 40 m. The resolution of the structures recorded in the profiles is 2 mm thickness. The structures drawn on the map record significant single cataclastic deformation bands (>5 mm thickness) and amalgamated multiple deformation bands, indicating the dominant orientations of deformation bands associated with the ramp. The locality of Figure 9 is indicated on the map.

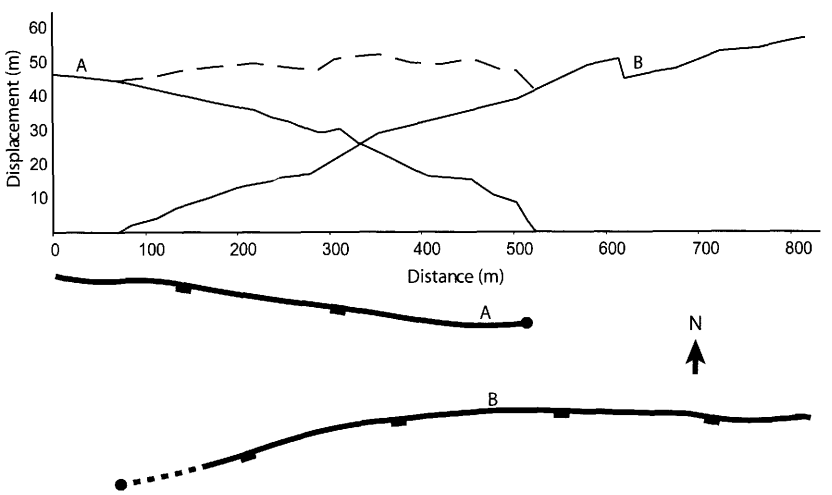

Fig. 5. Length–displacement diagram for the two main faults with a simplified sketch map of the two main faults bounding the relay ramp. The lines A and B represent the dip–slip displacement of each of the main faults, the faults being labelled correspondingly in the sketch map. The dashed line at the top of the diagram represents the total displacement of both faults along the length of the ramp.

Linking damage zone

The structural investigation of the relay ramp outcrop (the top unit cropping out on the surface being an aeolian dune unit of the Slickrock Mb) reveals a systematic pattern of largely cataclastic deformation bands in the ramp (Fig. 4). Several different orientations were identified and are described below. The bands are continuous features, and the different orientations frequently intersect, coalesce and overlap, thus forming an intricate network. In agreement with the findings of Antonellini & Aydin (1994, 1995), the deformation bands are most abundant close to the main faults bounding the ramp, and decrease in frequency away from the faults (Fig. 4). However, whereas north of the ramp the number of deformation bands decreases to zero some distance from the fault, the ramp area between the two bounding faults exhibits an overall abundance of cataclastic deformation bands in the range of 1–10 per metre as measured along north–south profiles. The area south of the ramp is affected by another fault located to the south and thus the number of deformation bands does not decrease here to the same extent as in the north.

Three main strike orientations of deformation bands were identified and are classified as follows (Fig. 6):

(1) ramp-parallel bands striking sub-parallel the bounding faults;
(2) ramp-diagonal bands striking obliquely to the bounding faults;
(3) curved bands strike sub-parallel to the bounding faults in the western part of the ramp, but deflect towards the south in the eastern part of the ramp, attaining NW–SE to north–south strikes.

All three categories display both synthetic and antithetic dip directions with respect to the bounding faults, and the bands typically dip at angles of 60–70°.

The ramp-parallel bands are abundant across the entire ramp, as well as north and south of the bounding faults, and make up the most common orientation of deformation bands. They form a significant portion of the high-intensity deformation band zones along the bounding faults (Figs 4 & 8). The ramp-parallel bands vary from single bands of 2–3 mm thickness to clusters of 100+ bands more than 10 cm wide (Fig. 7). Laterally continuous single deformation bands and clusters of 5–30

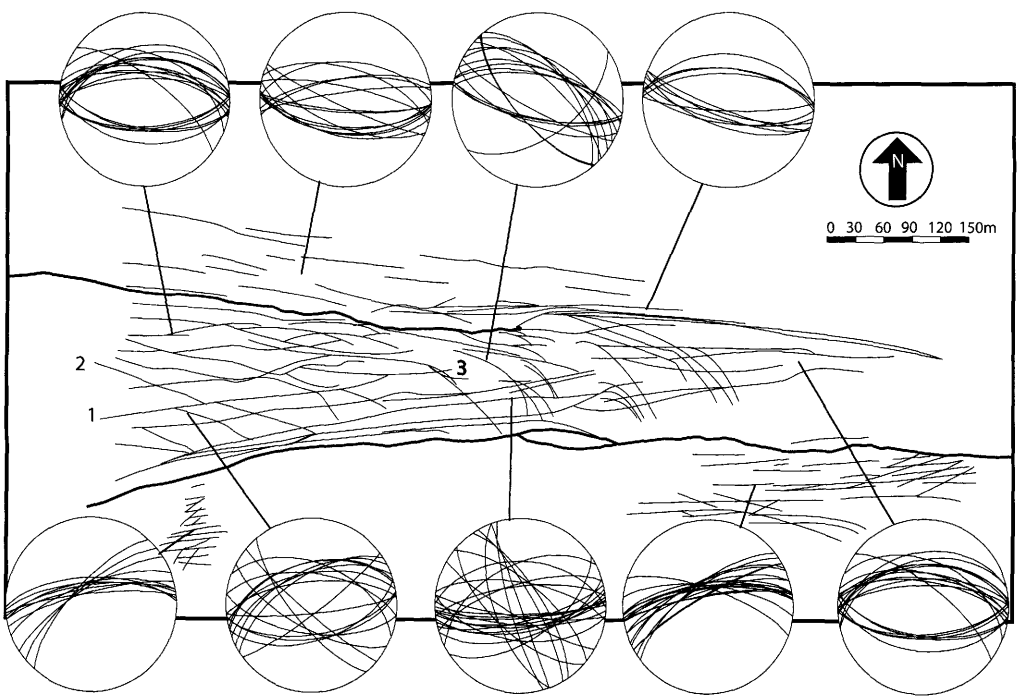

Fig. 6. Structural map and stereographic representation of cataclastic deformation band orientations at the Delicate Arch relay ramp. Examples of the three main orientations of bands are indicated with bold lines: (1) ramp-parallel bands; (2) ramp-diagonal bands; and (3) curved bands. The stereonets (equal area, lower hemisphere) show that the dominant strike orientation across the ramp is broadly east–west, but that deformation bands of *c*. NW–SE orientations often occur and are more common in certain parts of the ramp.

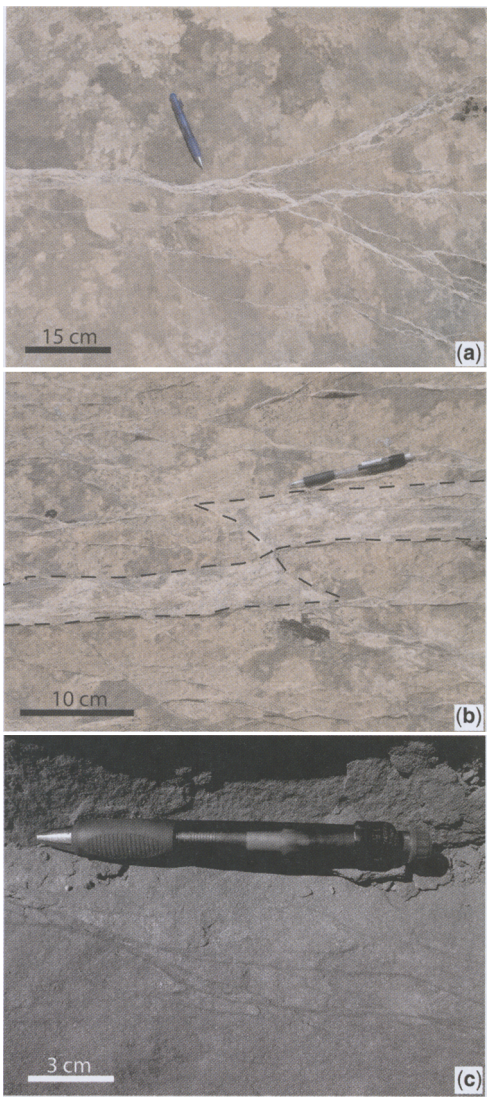

Fig. 7. Typical geometries of cataclastic deformation bands at the Delicate Arch ramp. (**a**) Clusters of deformation bands and single deformation bands forming a braided pattern as they join, part and intersect. (**b**) Intermediately thick deformation band cluster within a high-frequency network of bands near the southern bounding fault. The cluster is cross-cut and separated by younger deformation bands. (**c**) Framework phyllosilicate deformation bands in an interdune unit down section from the ramp surface.

bands are very common. Single bands can be traced for up to 100–150 m, and intersecting and amalgamating bands enable continuous coalesced structures to be traced along the entire length of the ramp. Displacement on single deformation bands is generally less than 1–2 cm, whereas large clusters of bands (>50) may display a total displacement of up to 20 cm.

Ramp-diagonal bands strike obliquely to the bounding faults. The most common orientation for these bands is NW–SE to WNW–ESE, but ENE–WSW to NE–SW striking bands also occur (Fig. 6). These two orientations are mutually intersecting (both cross-cut and displace each other). The ramp-diagonal bands exhibit the same varieties in extent, thickness and displacement as the ramp-parallel bands, yet the clusters do not grow as large (maximum 30–40 bands).

Curved bands (Fig. 8) display ramp-parallel (or ramp-diagonal) strikes in the western part of the ramp. Eastwards along strike, past the tip point of the northern bounding fault, they deflect towards the southern bounding fault and attain NW–SE to north–south strikes. These bands terminate at high (60–90°) angles to the southern bounding fault, either at the fault or some distance to the north of it. In some cases, bands that originate in the west with a *c*. east–west strike can be traced continuously along strike until they terminate at the southern bounding fault with a north–south orientation. The curved bands are laterally continuous, although less so than the ramp-parallel and ramp-diagonal bands. The thicknesses of the curved bands are also more modest, commonly featuring single bands of 0.5–3 mm thickness along with smaller clusters of *c*. 2–8 deformation bands.

Cross-cutting relationships between the three main orientations of deformation bands yield the following observations:

(1) Ramp-parallel, ramp-diagonal and curved bands are generally mutually cross-cutting; that is, every category of bands experiences displacement inflicted by the other two.
(2) Despite (1), ramp-parallel bands are the category that is most often cross-cut and displaced by the other two.
(3) Curved bands that are cross-cut and displaced by ramp-parallel bands are the least common situation.

The relay ramp's vertically stacked succession of aeolian, quartzose, clean, well-sorted dune units and muddier, more fine-grained interdune units provides an opportunity to investigate how the composition of the units affects the accommodation of deformation. Vertical sections of the ramp are well exposed, and it appears that the deformation bands are less continuous vertically than laterally (Schultz & Fossen 2002 suggest that this is typical for deformation bands in layered sequences). Cataclastic deformation bands in dune units are often seen to terminate at the interface of the muddier interdune units. However, some of the deformation bands can be traced continuously through several

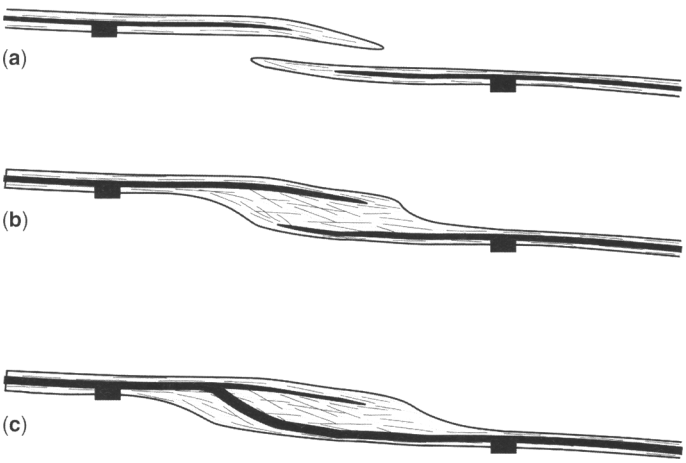

Fig. 8. Development of damage zone within and around a fault overlap structure. Three stages are shown. At the latter stage the faults are completely linked and behave as a single fault. The location of the former overlap zone is indicated by the bend in fault trace. See text for details.

dune and interdune units. The interdune units, having higher mud content, often display framework phyllosilicate deformation bands (Fig. 7c), which can occasionally be traced as the direct continuation of a cataclastic deformation band in a dune unit. However, the most important observation is that deformation bands are far less abundant in the interdune units than in the dune units. Furthermore, cataclasis is less common in the interdune units and the deformation bands are often of framework phyllosilicate or disaggregation type.

Whereas deformation of the Slickrock Mb has yielded abundant deformation bands (see below), the poorly sorted and less porous, fluvial deposits of the Morrison Fm (cropping out in the hanging wall of the southern main fault) are characterized by abundant, generally near fault-parallel, tension fractures. As the main focus of this paper is deformation in porous sandstones, these structures will not be described in detail here.

Discussion

Fault evolution through segment growth and linkage is currently a well accepted paradigm. The processes associated with the linkage of two fault segments can be described in a series of steps of under- and overlapping before the segments eventually coalesce (Peacock & Sanderson 1991, 1994; Fig. 8). As the tips of two segments grow towards each other, they pass from underlapping (Fig. 8a) to soft-linked overlapping (Fig. 8b), forming a relay ramp. The stress field and stress concentrations associated with the tips of the two fault segments interact and cause a complex pattern of deformation (Kattenhorn *et al.* 2000), as seen across the Delicate Arch Ramp. Eventually, if the faults continue to grow, the relay ramp will become breached, forming a hard-link overlap (breached relay; Fig. 8c) as the fault segments join. The previously separate fault segments thenceforth continue to slip as one single fault, and what was initially a relay ramp becomes a step in the fault trace.

The Delicate Arch Ramp is a soft-linked relay ramp and thus represents an intermediate step (Fig. 8b) in the history of two joining segments of a fault zone. As major movement along the fault zone ceased, the amalgamation of the two segments halted. The structural elements identified in association with the relay ramp portray a more complicated deformation pattern than the pattern commonly associated with damage zones of single faults (Berg 2004; Shipton & Cowie 2003). Whereas isolated faults in porous sandstones commonly produce damage zones with deformation bands dominantly striking sub-parallel to the main fault trend, this is not the case for the Delicate Arch Ramp. In the overlap area, the damage zone widens and envelopes the entire ramp (as seen in the intermediate stage of Fig. 8b), with several different orientations of deformation bands. The observations made of structural cross-cutting relationships at the ramp indicate that the formation of the differently orientated deformation bands was roughly coeval. However, a subtle age relationship between the different orientations may suggest that ramp-parallel bands were the first to form. It is clear, however, that when the northern fault was in the final stages of propagation to its current tip point, the faults were already overlapping. This is based on the diffraction

of the curved deformation bands towards the south. This probably happened due to the fact that the stress field became affected by the presence of the southern fault so that deformation bands bent towards this fault during their growth.

The tip damage zone of the northern fault shifts 30 m towards the north near the fault tip (Fig. 4). The reason for this could be the presence of a non-emergent fault in the sub-surface of the ramp (below the assumed tip damage zone). Thus, a small-scale early-stage relay structure associated with two overlapping faults may exist here (Fig. 4). This proto-relay does not display any curved bands (Fig. 4), which supports our suggestion that the curved bands form late during the development of ramp structures in this area. In fact, only deformation bands broadly parallel to the east–west trend of the main faults have been found to be associated with the proto-relay. This supports the theory that the ramp-parallel bands were the first to form.

Relay ramps, especially sub-seismic relays, are often quoted as a mechanism for fluid-flow communication within faulted reservoirs. Relays provide bed continuity within otherwise breached reservoir horizons and communication across faults which elsewhere reduce or stop flow. Published petrophysical studies of cataclastic deformation bands report 2–6 orders of magnitude permeability reduction across single bands (Antonellini & Aydin 1994; Ahlgren 2001; Fisher & Knipe 2001; Lothe *et al.* 2002). This implies that the deformation bands within damage zone enveloping the Delicate Arch Ramp could potentially restrict fluid flow through the ramp during production (assuming a similar ramp occurs in a petroleum reservoir). The following discussion will focus on evaluating the importance of this effect and the potential of relay ramps as flow paths across low-permeability fault zones.

A high frequency of low-permeability deformation bands (including clusters of deformation bands) broadly parallel to the ramp would significantly restrict fluid flow across the ramp in the north–south direction. However, assuming that the faults are sealing, we can, for the purpose of the evaluation of the relay ramp's flow potential, ignore north–south flow and focus on flow along the ramp in the east–west direction. For single faults with broadly fault-parallel structures in the damage zone, the permeability within the damage zone is expected to be much higher in the fault-parallel direction. However, the damage zone of the Delicate Arch ramp does not only display fault-parallel deformation bands. The ramp-diagonal and curved deformation bands cross-cutting and intersecting the ramp-parallel bands form an intricate web of compartments across the ramp (Fig. 6). This pattern operates at all scales and is repeated

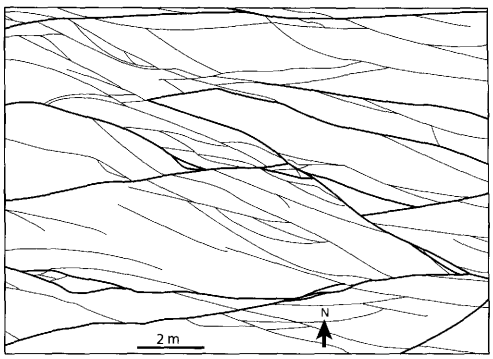

Fig. 9. A 10 × 14 m area of the western part of the ramp illustrates how the structural pattern and compartmentalization of the ramp are also featured at this scale. The thicker deformation bands are indicated with a thicker stroke. It should be noted that, even in the E–W direction, fluids would have to flow through several deformation bands just to pass this 10 × 14 m square, each representing a multiple-order magnitude reduction of permeability. The location of the outcrop is shown in Figure 4.

over the entire ramp area (Fig. 9). Thus, the damage zone could also potentially restrict fluid flow in the west–east (ramp-parallel) direction and trap migrating fluids during production. In an attempt to quantify this effect we will introduce some simple calculations in the following section.

Given that the contour map (Fig. 4) is based on data collected along north–south scanlines, the frequency per metre refers to the number of deformation bands crossed in that direction. Given that many of these are ramp-parallel bands that will not affect a particle of fluid running along (east–west) the ramp, it is necessary to know how many curved or diagonal bands need to be crossed. Figure 10a shows the relationship between deformation band frequency recorded by scanlines at different angles to two diagonal deformation bands. The relationship between the recorded structure frequencies of the two scanlines can be expressed by (see Fig. 10a):

$$\tan \alpha = B/A = \tan (90^\circ - \beta)$$

If the structure frequency is measured in deformation bands per metre along N–S profiles, we set $A = 1$ m, thus

$$B = \tan (90^\circ - \beta)$$

The ramp-diagonal bands on the Delicate Arch ramp display an average angle of 13° to the ramp

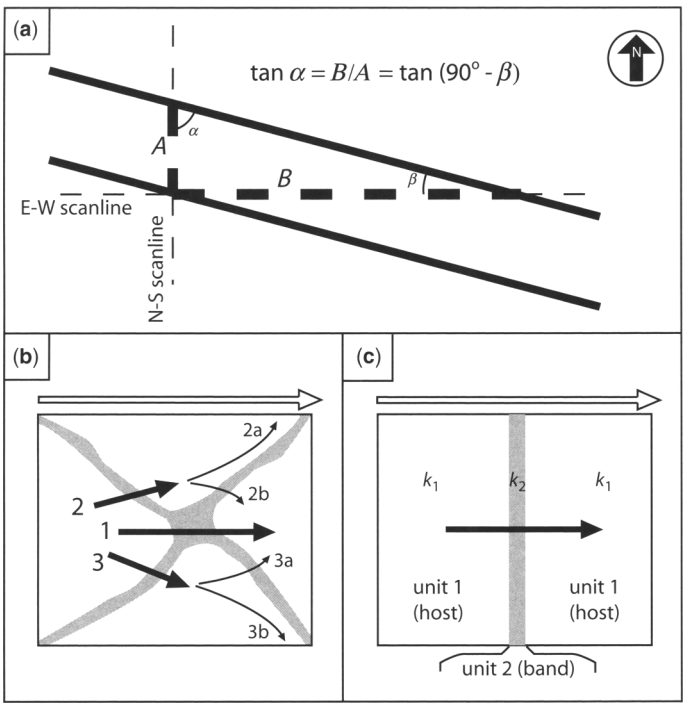

Fig. 10. (**a**) The relationship between structure frequency along two perpendicular scanlines, both of which cross two obliquely orientated deformation bands. (**b**) Possible flow paths for a particle of fluid flowing from the left to the right in a grid cell where two deformation bands cross-cut one another, forming a micro-trap. (**c**) As a minimum approximation, the harmonic average is applied to calculate the effective permeability for the situation in (b), considering each micro-trap the equivalent of one individual deformation band.

parallel bands (over the westernmost 400 m along a west → east scanline situated at equal distance from the main faults); thus, $\beta = 13^\circ$ and

$$B = \tan 77^\circ$$

Furthermore, there is a mid-ramp average of five deformation bands per metre along the N–S scanlines. Estimating that approximately 30% of the bands in this area are ramp-diagonal, the frequency of ramp-diagonal deformation bands along a west → east scanline is given by

$$F_{EW} = (0.3 \times F_{NS})/B = (0.3 \times 5)/\tan 77^\circ$$

where F_{EW} is the deformation band frequency recorded along an east–west scanline, F_{NS} the deformation band frequency recorded along a north–south scanline, and B is given in (Fig. 10a). The resulting deformation band frequency is 0.35 deformation bands per metre for the westernmost 400 m of the scanline. For the next 100 m eastward we estimate that 40% of the deformation bands as recorded along north–south profiles are ramp-diagonal or curved bands, here displaying a larger average angle to the ramp-parallel deformation bands; $\beta = 45^\circ$. F_{NS} averages 2 bands per metre in this area. This yields an F_{EW} of 0.8 deformation bands per metre. For simplicity we consider flow along the first 500 m of the ramp (from the west) to be sufficient to get around the faults, thus ignoring the potential effect of the process zone. The number of deformation bands that fluids would have to cross over the 500 m flow path is then given by

$$\begin{aligned}&(400\text{ m} \times 0.35\text{ bands/m})\\&\quad + (100\text{ m} \times 0.8\text{ bands/m})\\&\quad = 200\text{ bands}\end{aligned}$$

Most of these bands cross-cut and intersect the ramp-parallel bands, thus forming blind alleys, or mini-traps. If we conservatively assume that one-third of the diagonal and curved bands form such a mini-trap at the intersection with ramp-parallel bands (this is a minimum approximation as most of the diagonal bands intersect with other bands), we are left with about 73 individual mini-traps that fluids will have to cross.

Figure 10b shows a simple approximation for the possible flow paths for a fluid particle from the left to the right in a grid cell in which two deformation bands cross-cut one another. The flow paths representing the least hindrance to fluids are 2a and 3b (Fig. 10b). Therefore, as a minimum approximation we assume that each mini-trap represents a barrier equivalent to one individual band. This is an absolute minimum; more often than not it is observed that cross-cutting deformation bands lead to the development of more bands near the intersection (Fossen *et al.* 2005).

We calculate the effective permeability (K_{eff}) over a 500 m flowpath along the ramp (west → east) using the harmonic average for one-dimensional flow through an anisotropic medium, which is given by Cardwell and Parsons (1945):

$$K_{\text{eff}} = \frac{L}{\sum_{i=1}^{n} \frac{l_i}{k_i}}$$

where L is the total length of the flow path (500 m in our case), and l_i the accumulated width of unit i with bulk permeability k_i (Fig. 10c).

The results of the calculations are summarized in Table 1. The host rock permeability is set to 1000 mD (based on Antonellini & Aydin 1994), whereas permeability of single deformation bands is set to vary in the range of 0.1–100 mD (1–4 orders of magnitude less than that of the host rock). Furthermore, based on the presence of deformation band clusters (see above), we introduce one or more clusters in some of the calculation. We assume that clusters will represent the lowest values in the range of deformation band permeability, based on their continuity and thickness (up to 15–20 cm in some places). Thus, the permeability of the clusters is set to 1–2 orders of magnitude less than the single deformation band permeability and within the range of published values for cataclastic deformation bands (up to 6 orders of magnitude reduction relative to the host rock). Based on the observations from the Delicate Arch ramp, the clusters are regarded as continuous features that cross-cut each other, forming mini-traps in the same way single bands do. Calculations are made for an average 3 order reduction of permeability of single bands, and clusters with very low permeability (5 and 6 order reductions relative to the host rock). Single deformation band thickness is set at 2 mm, equal to the resolution of the contour map (Fig. 4); cluster thickness is set at 10 cm, a low average for the larger clusters mapped at the Delicate Arch ramp.

The results (Table 1) indicate that the presence of single deformation bands (not introducing any clusters) has no significant effect on the effective permeability due to the low total volume of deformation bands. Even at $K = 0.1$ mD for single bands, effective permeability is only reduced to about 255 mD over the entire flow path. Introducing one cluster (10 cm wide) at 2–4 order permeability reduction relative to the host rock has no dramatic effect on the effective permeability. However, introducing just one cluster with a 5 or 6 order reduction in permeability has a significant effect, yielding effective permeability values of *c.* 40 and 5 mD, respectively. Although gas might flow through a 5 mD sandstone, these values represent altogether very different reservoirs than the initial 1000 mD. In the last six calculations (Table 1) we look at how the systems is affected by clusters of very low permeability when the bulk permeability of single deformation bands is kept constant at 1 mD (at 3 order reduction of permeability, this represents a general average of published values). The effective permeability values now fall within a range of 0.5–16 mD, a reduction of the effective permeability by 2 to more than 3 orders of magnitude relative to the host rock. In comparison, the result with no clusters and 1 mD single deformation band permeability is an effective permeability of 774 mD.

These simple calculations indicate that:

(1) The permeability contrast between the structural heterogeneities and the host rock controls whether (and to what extent) the relay ramp would represent a conduit for fluid flow or not.
(2) Deformation bands and clusters displaying a 1–4 order reduction in permeability have only minor effects on effective permeability.
(3) Introducing very low-permeable clusters has a dramatic effect on the effective permeability.

Thus, the presence of continuous, very low-permeability zones in the ramp (in our case clusters of cataclastic deformation bands) largely controls the effective permeability. Although single deformation bands may only display a 1–3 order reduction of permeability, the presence of one single, continuous, very-low-permeability cluster of deformation bands impacts the effective permeability more than all of the single deformation bands combined. Thus, the important question to address is the presence of such low-permeability zones. For faults in the middle Jurassic Brent reservoirs in the North Sea, extremely low-permeability zones of framework phyllosilicate bands have been reported (up to 6 order permeability reduction; Fisher & Knipe 2001; Hesthammer & Fossen 2001). Thus, it is a viable option that relay ramps may feature this type of structural heterogeneity in existing oil and gas reservoirs.

Taking into account the variability in dip direction of the deformation bands (both synthetic and antithetic dips are common, see Fig. 6) it is likely that

Table 1. *Harmonic average calculations of the effective permeability along the Delicate Arch Ramp*

Host rock		Single deformation bands				Clusters				Total	
L_1 (host) m	K_1 (host) mD	Average thickness m	Number of DB to cross	L_2 (db) total m	K_2 (db) mD	Average thickness m	Number of clusters to cross	L_3 (cl) total m	K_3 (cl) mD	L_{tot} m	K_{eff} md
499.854	1000	0.002	73	0.146	100		0	—	—	500	997.379
499.754	1000	0.002	73	0.146	100	0.1	1	0.1	10	500	978.064
499.754	1000	0.002	73	0.146	100	0.1	1	0.1	1	500	831.651
499.854	1000	0.002	73	0.146	10	—	0	—	—	500	971.904
499.754	1000	0.002	73	0.146	10	0.1	1	0.1	1	500	813.863
499.754	1000	0.002	73	0.146	10	0.1	1	0.1	0.1	500	330.174
499.854	1000	0.002	73	0.146	1	—	0	—	—	500	774.169
499.754	1000	0.002	73	0.146	1	0.1	1	0.1	0.1	500	303.812
499.754	1000	0.002	73	0.146	1	0.1	1	0.1	0.01	500	46.967
499.854	1000	0.002	73	0.146	0.1	—	0	—	—	500	255.121
499.754	1000	0.002	73	0.146	0.1	0.1	1	0.1	0.01	500	41.807
499.754	1000	0.002	73	0.146	0.1	0.1	1	0.1	0.001	500	4.904
499.554	1000	0.002	73	0.146	1	0.1	3	0.3	0.01	500	16.316
499.554	1000	0.002	73	0.146	1	0.1	3	0.3	0.001	500	1.663
499.354	1000	0.002	73	0.146	1	0.1	5	0.5	0.01	500	9.873
499.354	1000	0.002	73	0.146	1	0.1	5	0.5	0.001	500	0.999
498.854	1000	0.002	73	0.146	1	0.1	10	1	0.01	500	4.968
498.854	1000	0.002	73	0.146	1	0.1	10	1	0.001	500	0.500

L_1, L_2 and L_3 are the total lengths (thicknesses) of host rock, deformation bands and clusters, respectively, along the flow path. K_1, K_2 and K_3 are the permeabilities of host rock, deformation bands and clusters, respectively. L_{tot} is the total length of the flow path and K_{eff} is the effective permeability. See text for details on the calculation of K_{eff}.

vertical fluid communication within the dune units will also be seriously affected. The deformation band network thus appears to be continuous in three dimensions (within the dune units). However, many of the deformation bands do not continue vertically from the aeolian sandstones into the interbedded interdune units. This suggests that, despite having lower permeabilities initially, the interdune units might act as a possible pathway for fluid flow. Cataclasis in the interdunes is not abundant, and the deformation bands present are predominantly of the framework phyllosilicate and disaggregation types. Although framework phyllosilicate bands are easily capable of three orders of magnitude permeability reduction, they are neither very continuous nor abundant in the study area (see above). A possible consequence of this is that the effective permeability is better in the interdune units than in the dune units, the inverse of what would be the case in a similar, but undeformed succession. Consequently, the relay ramp may still act as a conduit for flow across the fault zone. However, the bulk effective permeability will be lower than the host rock, given the reduction by the deformation bands and the flow through the lower-permeability facies. Thus, detailed knowledge of the stratigraphy of a subsurface reservoir is crucial in assessing the type of deformation structures likely to form at different levels in the stratigraphic column, which in turn controls the flow properties.

The compartmentalized nature of the ramp also calls for consideration of potential volumetric issues. If the isolated compartments of a ramp in the subsurface are included in the estimated producible reservoir volume, the economic potential of the reservoir could be overestimated, especially if the same error is repeated for a number of (overlapping) faults in the same reservoir. Thus, care should be taken to avoid including severely deformed fault zone volumes (such as relay ramps) when calculating producible reservoir volumes.

Production challenges related to fractured subsurface reservoirs are numerous and difficult, especially when dealing with deformation below seismic resolution (Edwards *et al.* 1993). Problems related to the production of reservoirs with deformation bands have been reported worldwide, e.g. the Nugget Sandstone reservoir unit in the Wyoming/Utah thrust belt (Lewis & Couples 1993), the Nubian Sandstone in Egypt (Harper & Moftah 1985), sandstone reservoirs offshore Nigeria (Olsson *et al.* 2004) and in the North Sea (Hesthammer & Fossen 2001).

Fault growth by segment linkage, similar to that documented in Utah, is common in the North Sea. This translates into numerous overlapping faults and relay ramps, which are well documented in the published literature (Fig. 11; Fossen & Hesthammer 1998*b*; Dawers & Underhill 2000; McLeod *et al.* 2000). Some studies address possible fluid flow through such structures (Hesthammer & Fossen

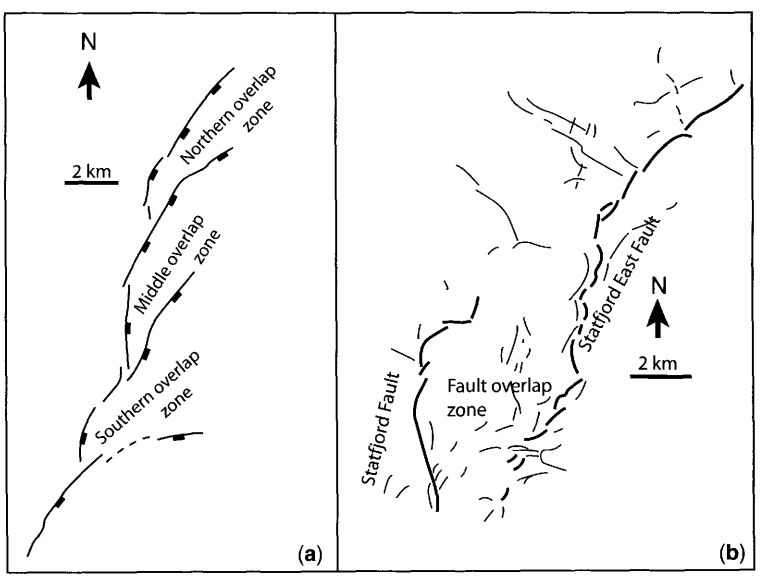

Fig. 11. (**a**) Fault structure at the top of the Heather Fm in the Statfjord East area in the East Shetland Basin, Northern North Sea. Three overlap zones are shown, with associated soft-linked and/or hard-linked relay ramps. Modified from Dawers & Underhill (2000). (**b**) Interpretation of main faults in the Statfjord–Statfjord East area showing a large-scale relay ramp between the overlapping Statfjord and Statfjord East Fault. Modified from Dawers & Underhill (2000).

1997, 2000; Manzocchi *et al.* 2004). Manzocchi *et al.* (2004) advocates the incorporation of sub-seismic relay zones into reservoir fault modelling by adjusting the fault transmissibility parameter to allow for increased across-fault flow, based on stochastic computation of relay zone occurrence in various structural settings. However, as this study demonstrates, there are important factors to consider that may reduce the fluid flow potential across a relay ramp. As mentioned previously, the internal deformation of relay ramps has not been examined elaborately in the literature, neither for cases in the North Sea nor elsewhere. This stresses the importance for a better understanding of these structures. Relay ramps may, as seen in this study, be complex zones displaying intense deformation that may hinder fluid flow. Thus, the general understanding of relay ramps as flow bridges across sealing faults may need some modification. If faults are sealing, relay ramps will, at least to some extent, be conduits for flow as they will generally have a higher permeability than the faults. However, the degree to which they are able to convey fluids from one compartment to another in a reservoir will depend on the structural heterogeneity of the ramp, and the permeability contrasts represented by this heterogeneity. In some reservoirs, the adjustment of the transmissibility parameter suggested by Manzocchi *et al.* (2004) is likely to overestimate the effect of relay ramps. More attention should therefore be paid to the local structural style associated with faults in a reservoir when adjusting the transmissibility parameters to account for relay ramps and across fault flow.

Whereas the damage zone of the Delicate Arch Ramp features abundant cataclastic deformation bands, this is generally not the case in the Jurassic reservoirs of the North Sea (Fisher & Knipe 2001, Hesthammer & Fossen 2001), which were deformed shortly after deposition. Although deformation bands are present, they are mainly of the disaggregation and framework phyllosilicate types. Disaggregation bands do not form coherent barriers to fluid flow, whereas framework phyllosilicate bands may reduce the effective permeability significantly (Hesthammer & Fossen 2000; Fisher & Knipe 2001). Thus, a controlling factor for seal potential is the mineral composition of the reservoir sand. Whereas faulting in clean sands would produce predominantly disaggregation deformation structures (provided the deformation occurs at shallow burial), a similar situation in a phyllosilicate-rich sand could result in abundant framework phyllosilicate bands or phyllosilicate smear (Fisher & Knipe 2001). As such, estimating the fluid flow potential across relay ramps in subsurface reservoirs requires an understanding of the mineral composition of the reservoir sand and the burial depth of the reservoir at the time of deformation, both of which control what type of sub-seismic heterogeneities will form within the ramp. Finally, it requires an understanding of the complex spatial distribution of deformation associated with overlapping faults, as exemplified in this paper. It is stressed that, although this is an example from one relay ramp, it is consistent with theoretical models of stress field orientations, perturbations and fracture patterns associated with laterally interacting faults (Kattenhorn *et al.* 2000). Thus, this study appears to provide a valid and representative picture of the distribution of small-scale deformation structures associated with relay ramps in extensional fault systems.

Finally, it should be noted that permeability reduction imposed by structural heterogeneity is only one out of several parameters that may influence flow negatively. Capillary effects, as well as increased tortuosity and a potential deterioration of sweep efficiency during production, also contribute to the total impact of structural heterogeneity on intra-ramp flow.

Summary and conclusions

The damage zone associated with the Delicate Arch ramp features a complex distribution of laterally continuous cataclastic deformation bands with three main orientations: ramp-parallel bands, ramp-diagonal bands and curved bands.

Intersection between deformation bands of different orientations may cause extensive compartmentalization and represent a major hindrance for fluid flow. However, the interdune units present in the study area, being less affected by deformation bands, may potentially act as a lower-permeability but less compartmentalized alternative (to the dune units) for fluid flow communication.

This study demonstrates that the overlapping of propagating normal fault segments increases the structurally complexity, and that large numbers of flow-impeding deformation features below seismic resolution may be present. Caution must be exercised when dealing with relay ramps in a reservoir setting. Although it is common (and often correct) to regard relay ramps in clastic reservoirs as efficient conduits for fluid flow when planning wells, the current study highlights a number of factors governing the sub-seismic deformation of the ramp that must be considered first. Variables such as depositional facies, mineral composition, structural style, deformation mechanisms, burial depth and distribution of strain control how relay ramps are formed and deformed. Three-dimensional-control of these factors is crucial in order to make sound estimates of relay ramp flow potential when planning wells. Combining the understanding of relay ramp internal deformation patterns with the available

data (such as seismic data, core data and regional data) is thus paramount for understanding the degree to which relay ramps will act as conduits for flow in a reservoir.

The distribution and importance (for fluid flow) of sub-seismic structural features associated with fault segment growth and linkage in subsurface reservoirs have so far not been sufficiently understood. Thus, the incorporation of such features in reservoir models is currently not satisfactory. Geological modelling and fluid flow simulation are therefore currently being undertaken in order to (a) better understand and quantify the structures' implications for fluid flow, and (b) suggest new and improved methods for incorporation of sub-seismic heterogeneities associated with fault overlap in reservoir modelling.

Are relay ramps conduits for fluid flow? Yes, relay ramps nearly always provide a better flow path for fluids than flow across a low-permeability fault itself. However, the degree to which relay ramps permit fluid flow is controlled by the above mentioned factors. This consideration must be included when fault transmissibilities are adjusted to allow for increased cross-fault flow in the presence of relays. If not, the effect of the relay ramps may be grossly overestimated.

References

AHLGREN, S. G. 2001. Exploring the formation, microtexture, and petrophysical properties of deformation bands in porous sandstone. *Bulletin of the American Association of Petroleum Geologists*, **85**, 2046.

ANTONELLINI, M. & AYDIN, A. 1994. Effect of faulting on fluid flow in porous sandstones: petrophysical properties. *Bulletin of the American Association of Petroleum Geologists*, **78**, 355–377.

ANTONELLINI, M. & AYDIN, A. 1995. Effect of faulting on fluid flow in porous sandstones: geometry and spatial distribution. *Bulletin of the American Association of Petroleum Geologists*, **79**, 642–671.

ANTONELLINI, M., AYDIN, A. & POLLARD, D. D. 1994. Microstructure of deformation bands in porous sandstones at Arches National Park, Utah. *Journal of Structural Geology*, **16**, 941–959.

AYDIN, A. 1978. Small faults formed as deformation bands in sandstone. *Pageoph*, **116**, 913–930.

AYDIN, A. & JOHNSON, A. M. 1978. Development of faults as zones of deformation bands and as slip surfaces in sandstone. *Pageoph*, **116**, 931–942.

BERG, S. S. 2004. *The architecture of normal fault zones in sedimentary rocks: analyses of fault core composition, damage zone asymmetry, and multiphase flow properties*. Ph.D. dissertation, University of Bergen.

CARDWELL, W. T. & PARSONS, R. I. 1945. Average permeability of heterogeneous sands. *Transactions of the American Institute of Mining Engineers*, **160**, 34–42.

CARTWRIGHT, J. A., MANSFIELD, C. S. & TRUDGILL, B. D. 1996. Fault growth by segment linkage. *In*: BUCHANAN, P. C. & NIEUWLAND, D. A. (eds) *Modern Developments in Structural Interpretations*. Geological Society, London, Special Publications, **99**, 163–177.

CHILDS, C., WATTERSON, J. & WALSH, J. J. 1995. Fault overlap zones within developing normal fault systems. *Journal of the Geological Society, London*, **152**, 535–549.

COWIE, P. A. & SHIPTON, Z. K. 1998. Fault tip displacement gradients and process zone dimensions. *Journal of Structural Geology*, **20**, 983–997.

CRUIKSHANK, K. M. & AYDIN, A. 1995. Unweaving the joints in Entrada Sandstone, Arches National Park, Utah, U.S.A. *Journal of Structural Geology*, **17**, 409–421.

DAVATZES, N. C. & AYDIN, A. 2003. Overprinting faulting mechanisms in high porosity sandstones of SE Utah. *Journal of Structural Geology*, **25**, 1795–1813.

DAWERS, N. H. & UNDERHILL, J. R. 2000. The role of fault interaction and linkage in controlling synrift stratigraphic sequences: late Jurassic, Statfjord East Area, northern North Sea. *Bulletin of the American Association of Petroleum Geologists*, **84**, 45–64.

DOELLING, H. H. 1985*a*. *Geologic map of Arches National Park and vicinity, Grand County, Utah*. Utah Geological and Mineral Survey, Map **74**.

DOELLING, H. H. 1985*b*. *Geology of Arches National Park. Utah Geological and Mineral Survey*.

DOELLING, H. H. 2001. *Geologic map of the Moab and eastern part of the San Rafael Desert 30′ × 60′ quadrangles, Grand and Emery Counties, Utah, and Mesa County, Colorado*. Utah Geological Survey, Map **180**.

DURLOFSKY, L. J. 1992. Modeling fluid flow through complex reservoir beds. *Society of Petroleum Engineers Formation Evaluation*, **7**, 315–322.

EDWARDS, H. E., BECKER, A. D. & HOWELL, J. A. 1993. Compartmentalization of an aeolian sandstone by structural heterogeneities: Permo-Triassic Hopeman Sandstone, Moray Firth, Scotland. *In*: NORTH, C. P. & PROSSER, D. J. (eds) *Characterization of Fluvial and Aeolian Reservoirs*. Geological Society, London, Special Publications, **73**, 339–366.

FISHER, Q. J. & KNIPE, R. J. 2001. The permeability of faults within siliciclastic petroleum reservoirs of the North Sea and Norwegian Continental Shelf. *Marine and Petroleum Geology*, **18**, 1063–1081.

FOSSEN, H. 2003. Fault linkage in the horizontal direction. *EAGE Learning Geoscience* (www.learninggeoscience.net).

FOSSEN, H. & HESTHAMMER, J. 1997. Geometric analysis and scaling relations of deformation bands in porous sandstone. *Journal of Structural Geology*, **19**, 1479–1493.

FOSSEN, H. & HESTHAMMER, J. 1998*a*. Deformation bands and their significance in porous sandstone reservoirs. *First Break*, **16**, 21–25.

FOSSEN, H. & HESTHAMMER, J. 1998*b*. Structural geology of the Gullfaks Field, northern North Sea. *In*: COWARD, M. P., DALTABAN, T. S. & JOHNSON, H. (eds) *Structural Geology in Reservoir*

Characterization Geological Society, London, Special Publications, **127**, 231–261.

FOSSEN, H., JOHANSEN, T. E. S., HESTHAMMER, J. & ROTEVATN, A. 2005. Fault interaction in porous sandstone and implications for reservoir management; examples from Southern Utah. *Bulletin of the American Association of Petroleum Geologists*, **89**, 1593–1606.

HARPER, T. R. & MOFTAH, I. 1985. Skin effect and completion options in the Ras Budran Reservoir. *SPE*, **13708**, 211–226.

HESTHAMMER, J. & FOSSEN, H. 1997. Seismic attribute analysis in structural interpretation of the Gullfaks Field, northern North Sea. *Petroleum Geoscience*, **3**, 13–26.

HESTHAMMER, J. & FOSSEN, H. 2000. Uncertainties associated with fault sealing analysis. *Petroleum Geoscience*, **6**, 37–45.

HESTHAMMER, J. & FOSSEN, H. 2001. Structural core analysis from the Gullfaks area, northern North Sea. *Marine and Petroleum Geology*, **18**, 411–439.

HESTHAMMER, J., BJØRKUM, P. A. & WATTS, L. 2002. The effect of temperature on sealing capacity of faults in sandstone reservoirs: examples from the Gullfaks and Gullfaks Sør fields, North Sea. *Bulletin of the American Association of Petroleum Geologists*, **86**, 1733–1751.

IMBER, J., TUCKWELL, G. W. *ET AL.* 2004. Three-dimensional distinct element modelling of relay growth and breaching along normal faults. *Journal of Structural Geology*, **26**, 1897–1911.

KATTENHORN, S. A., AYDIN, A. & POLLARD, D. D. 2000. Joints at high angles to normal fault strike: an explanation using 3-D numerical models of fault-perturbed stress fields. *Journal of Structural Geology*, **22**, 1–23.

KIM, Y.-S., PEACOCK, D. C. P. & SANDERSON, D. J. 2004. Fault damage zones. *Journal of Structural Geology*, **26**, 503–517.

KNIPE, R. J. 1997. Juxtaposition and seal diagrams to help analyze fault seals in hydrocarbon reservoirs. *Bulletin of the American Association of Petroleum Geologists*, **81**, 187–195.

LEWIS, H. & COUPLES, G. D. 1993. Production evidence for geological heterogeneities in the Anschutz Ranch East Field, western USA. *In*: NORTH, C. P. & PROSSER, D. J. (eds) *Characterization of Fluvial and Aeolian Reservoirs*. Geological Society, London, Special Publications, **73**, 321–338.

LOTHE, A. E., GABRIELSEN, R. H., BJØRNEVOLL-HAGEN, N. & LARSEN, B. T. 2002. An experimental study of the texture of deformation bands; effects on the porosity and permeability of sandstones. *Petroleum Geoscience*, **8**, 195–207.

MAIR, K., MAIN, I. & ELPHICK, S. 2000. Sequential growth of deformation bands in the laboratory. *Journal of Structural Geology*, **22**, 25–42.

MANSFIELD, C. S. & CARTWRIGHT, J. A. 2001. Fault growth by linkage: observations and implications from analogue models. *Journal of Structural Geology*, **23**, 745–763.

MANZOCCHI, T., HEATH, A. E., WALSH, J. J., CHILDS, C. & BAILEY, W. R. 2004. *Faults in conventional flow models: an investigation of numerical and geological assumptions*. Annex 8 of the Final Technical Report for the SAIGUP project (EU Project number NNE5-2000-20095).

MCLEOD, A. E., DAWERS, N. H. & UNDERHILL, J. R. 2000. The propagation and linkage of normal faults: insights from the Strathspey–Brent–Statfjord fault array, northern North Sea. *Basin Research*, **12**, 263–284.

OLSSON, W. A., LORENZ, J. C. & COOPER, S. P. 2004. A mechanical model for multiply-oriented conjugate deformation bands. *Journal of Structural Geology*, **26**, 325–338.

PEACOCK, D. C. P. 2003. Scaling of transfer zones in the British Isles. *Journal of Structural Geology*, **25**, 1561–1567.

PEACOCK, D. C. P. & SANDERSON, D. J. 1991. Displacements, segment linkage and relay ramps in normal fault zones. *Journal of Structural Geology*, **13**, 721–733.

PEACOCK, D. C. P. & SANDERSON, D. J. 1994. Geometry and development of relay ramps in normal fault systems. *Bulletin of the American Association of Petroleum Geologists*, **78**, 147–165.

RYKKELID, E. & FOSSEN, H. 2002. Layer rotation around vertical fault overlap zones: observations from seismic data, field examples and physical experiment. *Marine and Petroleum Geology*, **19**, 181–192.

SCHULTZ, R. A. & FOSSEN, H. 2002. Displacement-length scaling in three dimensions: the importance of aspect ratio and application to deformation bands. *Journal of Structural Geology*, **24**, 1389–1411.

SHIPTON, Z. K. & COWIE, P. A. 2003. A conceptual model for the origin of fault damage zone structures in high-porosity sandstone. *Journal of Structural Geology*, **25**, 333–344.

STERNLOF, K. R., CHAPIN, J. R., POLLARD, D. D. & DURLOFSKY, L. J. 2004. Permeability effects of deformation band arrays in sandstone. *Bulletin of the American Association of Petroleum Geologists*, **88**, 1315–1329.

WEBER, K. J. 1987. Computation of initial well productivities in aeolian sandstone on the basis of a geological model, Leman gas field, U.K. *In*: TILLMAN, R. W. & WEBER, K. J. (eds) *Reservoir Sedimentology*. Society of Economic Paleontologists and Mineralogists Special Publications, **40**, 333–354.